Cell Death and Differentiation (2007) 14, 1647–1656

www.nature.com/cdd

Mdm38 protein depletion causes loss of mitochondrial K^+/H^+ exchange activity, osmotic swelling and mitophagy

K Nowikovsky[1], S Reipert[2], RJ Devenish[3] and RJ Schweyen*,[1]

Loss of the *MDM38* gene product in yeast mitochondria results in a variety of phenotypic effects including reduced content of respiratory chain complexes, altered mitochondrial morphology and loss of mitochondrial K^+/H^+ exchange activity resulting in osmotic swelling. By use of doxycycline-regulated shut-off of *MDM38* gene expression, we show here that loss of K^+/H^+ exchange activity and mitochondrial swelling are early events, associated with a reduction in membrane potential and fragmentation of the mitochondrial reticulum. Changes in the pattern of mitochondrially encoded proteins are likely to be secondary to the loss of K^+/H^+ exchange activity. The use of a novel fluorescent biosensor directed to the mitochondrial matrix revealed that the loss of K^+/H^+ exchange activity was immediately followed by morphological changes of mitochondria and vacuoles, the close association of these organelles and finally uptake of mitochondrial material by vacuoles. Nigericin, a K^+/H^+ ionophore, fully prevented these effects of Mdm38p depletion. We conclude that osmotic swelling of mitochondria triggers selective mitochondrial autophagy or mitophagy.
Cell Death and Differentiation (2007) **14,** 1647–1656; doi:10.1038/sj.cdd.4402167; published online 1 June 2007

Mitochondria are dynamic organelles in morphology and turnover. They form a branched, tubular network located below the cell cortex in budding yeast. In growing cells this network is a highly motile structure. Equilibrium between fission and fusion of tubular branches is essential for cellular adaptation to varying physiological conditions and to ensure inheritance of mitochondria by daughter cells.[1,2] These processes involve a series of proteins that have to deal with joining or separating both the outer and inner mitochondrial membranes in a coordinated fashion. Maintenance and inheritance of mitochondria also involve active movement along cytoskeletal elements.[3] Mutants with defects in the fusion process contain numerous spherical fragmented mitochondria. In contrast, fission defects result in net-like agglomerations of mitochondria.[1] There is growing support for the role of ion homeostasis in determining mitochondrial morphology. Recent work points to a crucial role of mitochondrial Ca^{2+} homeostasis in shaping mitochondria. Changes of intramitochondrial Ca^{2+} concentration and in Ca^{2+} signaling between ER and mitochondria trigger mitochondrial fragmentation at an early stage of cell death.[4]

Systematic analysis of a yeast deletion mutant collection has led to the identification of a large series of genes as being directly or indirectly involved in shaping mitochondrial morphology.[5] One of those genes, *MDM38/YOL027c*, also showed up in a screen for genes involved in mitochondrial cation homeostasis. Its product is an integral protein of the inner mitochondrial membrane, and is well conserved among all eukaryotes.[6] Hemizygous deletion in humans has been invoked as causing a major part of the Wolf–Hirschhorn disease phenotype.[7] The presence of a putative EF Ca^{2+} binding hand domain within almost all Mdm38p homologues suggested a role for Mdm38p in mitochondrial Ca^{2+} homeostasis and morphology.[5,8] We have recently characterized Mdm38p/Mkh1p as an essential component of the mitochondrial K^+/H^+ exchange system. Mutants deleted for this gene have functional defects of mitochondria, reduced growth of cells on non-fermentable substrate (*petite* phenotype), a nearly complete loss of mitochondrial $K^+(Na^+)/H^+$ exchange activity, high K^+ matrix content, low membrane potential ($\Delta\psi$), and dramatically increased volume.[6,9] Recently, Frazier *et al.* (2006) noted reduced amounts of certain mitochondrially encoded proteins in the inner membrane despite their translation efficiency being unchanged. They found that protein A-tagged Mdm38p formed complexes with mitochondrial ribosomes, and suggested that the reduced amount of some of the mitochondrially encoded proteins of complexes III, IV, and V resulted from the lack of Mdm38p interacting with mitochondrial ribosomes to mediate membrane insertion of several proteins of nuclear and mitochondrial origin.[10] These data led Frazier et *al.* to propose that Mdm38p is acting as a component of the mitochondrial protein export machinery.

[1]Department of Genetics, Max F Perutz Laboratories, University of Vienna, Vienna, Austria; [2]Department of Molecular Cell Biology, Max F Perutz Laboratories, University of Vienna, Vienna, Austria and [3]Department of Biochemistry and Molecular Biology, and the ARC Centre of Excellence in Structural and Functional Microbial Genomics, Monash University, Clayton campus, Victoria, Australia
*Corresponding author: RJ Schweyen, Department of Genetics, Max F Perutz Laboratories, University of Vienna, Dr. Bohr Gasse 9, Vienna A-1030, Austria.
Tel: +43 1 42 77 54604; Fax: +43 1 4277 9546; E-mail: rudolf.schweyen@univie.ac.at
Keywords: K^+/H^+ exchange; MDM38; mitophagy; osmotic swelling
Abbreviations: $\Delta\psi$, membrane potential; dox, doxycycline; FCCP, carbonylcyanide-*p*-trifluoromethoxyphenylhydrazone; JC-1, 5,5′,6,6′-tetrachloro-1,1′,3,3′-tetraethylbenzimidazolocarbocynine iodide; KOAc, potassium acetate; RFP, red fluorescent protein
Received 07.11.06; revised 04.4.07; accepted 05.4.07; Edited by G Kroemer; published online 01.6.07

Making use of a yeast strain conditionally expressing Mdm38p, we address the following questions. Which is the primary phenotype arising from the deletion of *MDM38*? Is the reduction of mitochondrial-encoded proteins a direct effect of the lack of Mdm38p, or a secondary consequence resulting from the disturbance of mitochondrial K^+ homeostasis, swelling and/or reduction in $\Delta\psi$? Since we observed mitochondrial fragmentation upon Mdm38p shut-off, and the association of mitochondrial fragments with vacuoles, we asked whether breakdown of the mitochondrial reticulum due to osmotic swelling led to mitochondria-selective autophagy, which has been termed mitophagy.[11,12]

Results

Disturbance of mitochondrial translation and membrane insertion is not a primary effect of *mdm38*Δ. Yeast strains disrupted for the *MDM38* gene (*mdm38*Δ) exhibit a growth defect on non-fermentable substrate (*petite* phenotype) and altered mitochondrial morphology,[5] reduced amounts of certain mitochondrially encoded proteins, reduced $\Delta\psi$[6,13] and a near total loss of mitochondrial K^+/H^+ exchange activity associated with increased K^+ content and osmotic swelling.[6,9] Figure 1 presents the pattern of mitochondrially translated proteins obtained by incubation of wild type and *mdm38*Δ cells with labeled methionine in the presence of cycloheximide. Consistent with previous observations,[13] we observe a reduction in abundance of Cox2, Cob, and Cox3, but no apparent changes in ATP synthase proteins. Cytochrome spectra also revealed reductions in the bc1 and a.a3 spectral bands (data not shown). Similar results were obtained when we compared the levels of mitochondrial membrane proteins as detected by BN gel electrophoresis and immunoblotting (Supplementary Figure S1). Addition of nigericin, a K^+/H^+ ionophore, to *mdm38*Δ cells efficiently restored both growth of these cells on non-fermentable substrate (Figure 2) and the pattern of mitochondrially synthesized proteins (Figure 1). These results are difficult to reconcile with the suggestion that the primary role of Mdm38p is in the insertion of proteins from the mitochondrial matrix into the inner membrane.[13] Rather, they support our proposal that a lack of K^+/H^+ activity causes the *mdm38*Δ growth defect[6] and that effects on the pattern of mitochondrially synthesized proteins are a result thereof.

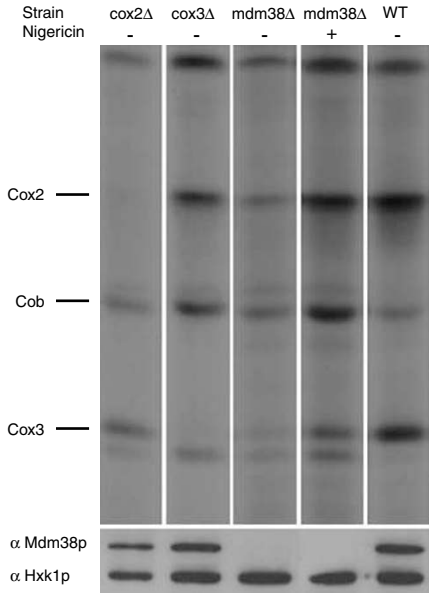

Figure 1 Effects of the *mdm38*Δ mutation on the expression pattern of mitochondrially encoded proteins. Upper panel: Cultures of *cox2*Δ, *cox3*Δ, and *mdm38*Δ mutant and wild-type cells were grown and pulse-labeled with ^{35}S-methionine in the presence of cycloheximide as described under 'Materials and Methods'. *mdm38*Δ cells were grown in the presence or the absence of nigericin as indicated. Total cell protein (15 μl loaded per fraction) was separated by 16% SDS-PAGE and subsequently analyzed by autoradiography. The *mit*$^-$ *cox2* and cox*3*Δ strains serve as reference to identify cox2p and cox3p bands. Lower panel: immunoblots of the same protein extractions as shown in the upper panel (5 μl loaded per fraction) were probed in parallel with an Mdm38p antiserum and with hexokinase (Hxk1p) antiserum serving as a loading control

To differentiate further between primary and secondary phenotypic effects of the *mdm38*Δ mutation, we ectopically expressed the *MDM38* gene under the control of a doxycycline (dox) regulated promoter in an *mdm38*Δ deletion strain (designated *MDM38*^{dox}). As shown in Figure 3 (upper panel), the amount of Mdm38p decreased below the level of detection within 25 h (t_{25}) following downregulation of its expression. The pattern of mitochondrially synthesized proteins observed with pulse labeling assays, however, remained essentially unchanged up to 50 h following downregulation (Figure 3, lower panel). Equally, steady-state levels of mitochondrially encoded Cox subunits remained constant for up to 50 h following *MDM38* downregulation (Supplementary Figure S2). In addition, cytochrome bc1 and a.a3 spectral bands were comparable to those of wild-type cells up to 50 h following Mdm38p downregulation (not shown).

Primary effects of *mdm38*Δ mutation on mitochondrial K^+/H^+ exchange activity. Having established that reduction in the amount of mitochondrial proteins is not an immediate effect of the *MDM38* gene deletion, we sought to determine its primary effect. For this purpose, we carried out further series of time-course experiments, making use of the *MDM38*^{dox} strain.

Hypoosmotic potassium acetate (KOAc) treatment of wild-type mitochondria results in rapid swelling, which reflects

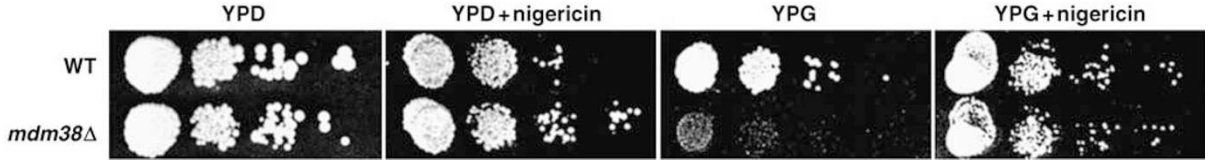

Figure 2 Suppression of the *mdm38*Δ growth phenotype by nigericin. Serial dilutions of wild type and *mdm38*Δ strains were spotted onto fermentable (YPD) and non-fermentable (YPG) media containing or lacking nigericin (2 μM) as indicated. YPD plates were incubated at 28°C for 3 days, YPG plates for 5 days

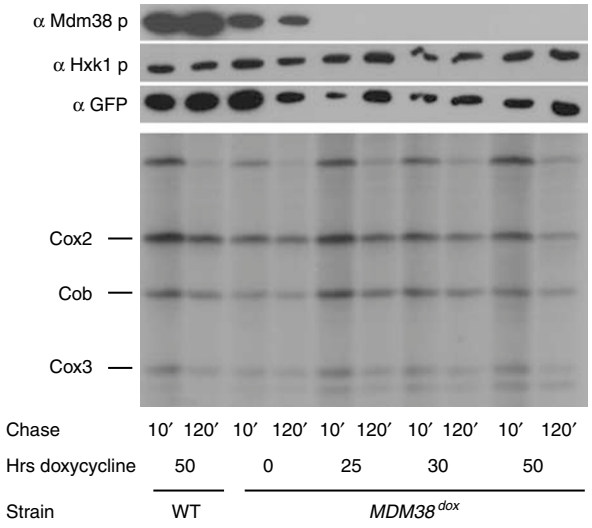

Figure 3 Synthesis of mitochondrial proteins continues during Mdm38p depletion. Mutant *mdm38*Δ cells expressing Mdm38p under the control of dox from a CEN plasmid pCM189 (*MDM38*^{dox}) and wild-type cells carrying the same plasmid without the *MDM38* gene (WT) were grown in SGal medium in the presence or the absence of dox for up to 50 h. Cells were kept in logarithmic growth phase by daily re-dilutions. Cells were harvested at indicated times following ^{35}S-methionine labeling in the presence of cycloheximinde (as indicated in Figure 1, except that the duration of the chase was either 10 or 120 min), proteins were separated using 16% SDS-PAGE. Upper panel: samples (5 μl loaded per fraction) were immunodecorated with an Mdm38p antiserum to observe dox-induced depletion or with GFP or hexokinase (Hxk1p) antisera (loading control). Lower panel: autoradiography of same samples (15 μl loaded per fraction)

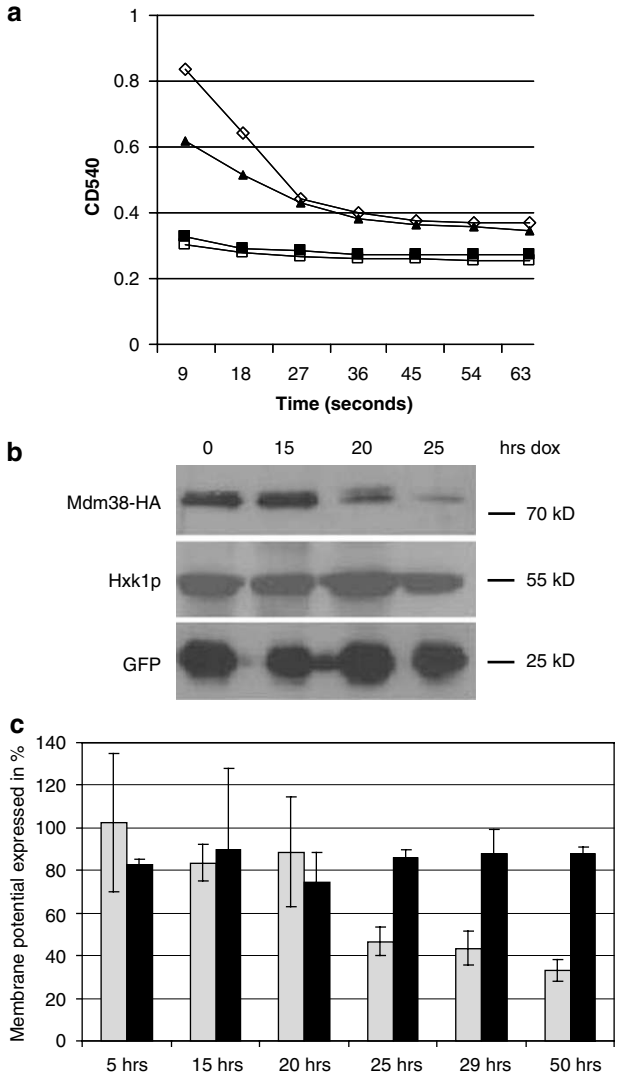

Figure 4 Loss of K^+/H^+ exchange activity and $\Delta\psi$ correlate with Mdm38p depletion. *MDM38*^{dox} cells and wild-type cells expressing the *tetO* promoter from the empty plasmid pCM189 (WT) were transformed with pYX232-mtGFP and grown in SGal-medium in the presence of dox for up to 50 h. (**a**) KOAc induced swelling of mitochondria isolated from *MDM38*^{dox} cells at various times of dox treatment was measured as a decrease of OD_{540}. Duration of dox treatment was –◇– 5 h, –▲– 20 h, –■– 25 h, –□– 50 h. (**b**) Depletion of Mdm38p was monitored by Western blotting. Hxk1p and mitochondrially targeted GFP served as loading controls. (**c**) Mitochondrial $\Delta\psi$ was determined by JC-1 staining. Shown are mean values of three measurements expressed individually as percentage of the maximum and the minimum obtained by hyperpolarization with nigericin and depolarization with FCCP, respectively. Black bars WT, grey *MDM38*^{dox}. Error bars represent S.D.

K^+/H^+ exchange activity.[14] It can be observed as a decrease in light absorbance of mitochondrial suspensions. As described in our previous studies,[6] mutant *mdm38*Δ mitochondria exhibit severely reduced KOAc-induced swelling in contrast to wild-type mitochondria. Mitochondria isolated from *MDM38*^{dox} cells initially (up to t_{16} of Mdm38p depletion) displayed a high swelling amplitude (Figure 4a). At later times, following dox-mediated shut-off of Mdm38p expression the swelling amplitude reached first intermediate levels (t_{20}), then became marginal (t_{25} to t_{50}). This correlates with the level of Mdm38 protein at these time points (Figure 4b). Mitochondria of wild-type cells treated similarly with dox for a time period up to t_{50} did not show any significant change of their swelling amplitude (data not shown). These results are consistent with a primary role of Mdm38p in K^+/H^+ exchange.

As a further parameter, we determined the mitochondrial $\Delta\psi$ from the same preparations used for swelling and immunoblotting experiments (Figure 4a and b, respectively). Mdm38p depletion resulted in a decrease of $\Delta\psi$ starting at t_{25} (Figure 4c) while dox treatment of wild-type cells did not show any reduction in $\Delta\psi$.

Ultrastructural changes of cell organelles in Mdm38-depleted cells. As shown previously by electron microscopy, one hallmark of *mdm38*Δ cells is drastically enlarged mitochondria that are nearly devoid of cristae structures and have reduced electron density.[6] This phenotype is in accordance with a defect in K^+/H^+ exchange activity, increased K^+ content and osmotic swelling.[6,9] Here, we observed changes in mitochondrial and vacuolar morphology resulting from gradual depletion of Mdm38p in *MDM38*^{dox} cells. As soon as K^+/H^+ exchange activity became low (beginning with t_{25} Mdm38p depletion), we observed spherical mitochondria with low electron density and few remnants of internal membrane structures (cristae) (Figure 5a, middle panel). Most interestingly, mitochondria appeared to be closely associated with the vacuole. The

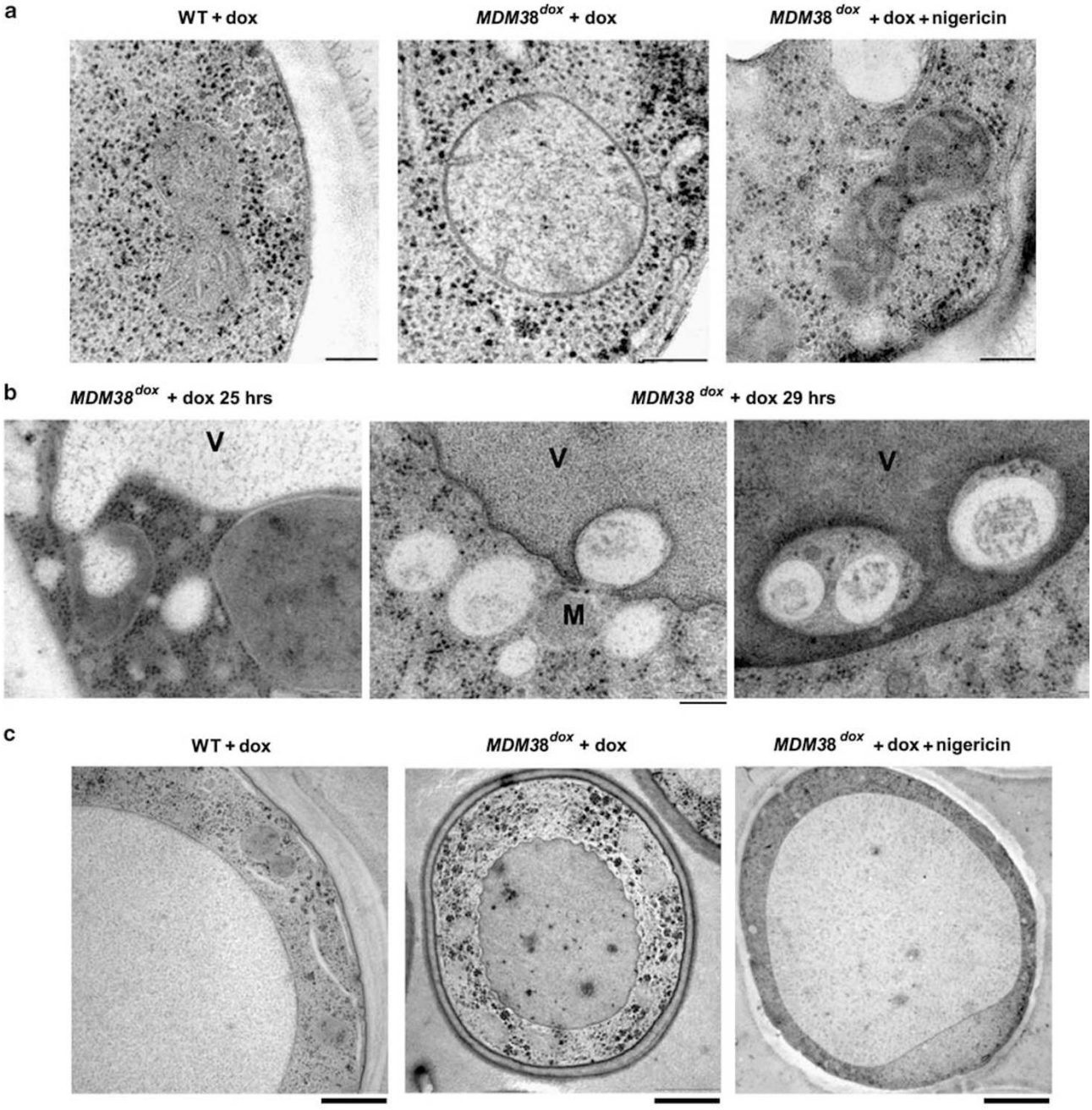

Figure 5 Changes in mitochondrial morphology of *MDM38*^{dox} cells after downregulation of Mdm38p and following addition of nigericin. Electron micrographs were prepared from cells grown to early logarithmic phase ($OD_{600} = 0.5$) in SGal-medium in the presence of dox when indicated. (**a**) Comparison of mitochondria from a wild-type strain expressing the *tetO* promoter from the empty plasmid pCM189 (WT, left) cell, a *MDM38*^{dox} cell grown for 29 h in the presence of dox (middle), a *MDM38*^{dox} cell grown for 29 h in the presence of dox and nigericin added for the final 5 h of the growth period (right) scale bars: 200 nm. (**b**) Interactions between vacuoles and mitochondria in *MDM38*^{dox}. Vacuolar extension towards mitochondria dox treatment for 25 h (left); Mitochondrial particles with low electron density in proximity of vacuole membrane indentations (middle); mitochondrial particles engulfed by vacuoles, dox treatment for 29 h (right). Scale bar: 200 nm. (**c**) Structure of mitochondria (M) and vacuole (V) in wild-type (WT, left) and *MDM38*^{dox} cells grown in presence of dox and in absence (middle) or presence (right) of nigericin. Scale bar (left) 0.5 μm, (middle and right) 1 μM

electron density of the vacuolar membrane was strongly increased and exhibited concave indentations all over (Figure 5b, middle panel and Figure 5c, middle panel). These vacuolar membrane formations have previously been described to occur in mitophagy.[11,15,16] In fact, at t_{25} of Mdm38p depletion vacuoles appeared to protrude towards mitochondria and the electron density of both interacting organelles was strongly reduced (Figure 5b, left panel). Ongoing proteolysis could be a possible explanation for this phenomenon. Mitochondrial particles exhibiting low electron density were eventually engulfed by the vacuoles together with or without surrounding cytoplasm (Figure 5b, right

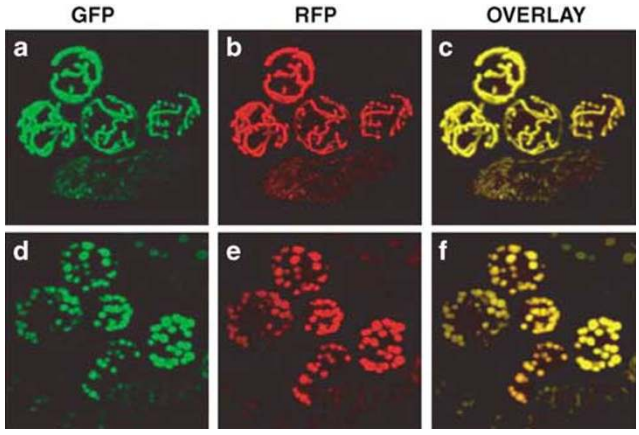

Figure 6 Disturbed mitochondrial morphology in *mdm38*Δ cells. Wild type (**a–c**) and *mdm38*Δ cells (**d–f**) were transformed with pVT100U-mtGFP,[18] grown on SGal-ura medium to early exponential phase, stained with 0.5 μM rhodamine B hexyl ester and visualized by laser confocal microscopy. (**a**) and (**d**) GFP fluorescence, (**b**) and (**e**) rhodamine fluorescence, (**c**) and (**f**) overlay of GFP and rhodamine fluorescence

panel). Cells exhibiting these particular features of mitochondria and vacuoles were abundant at t_{25} to t_{29} of the Mdm38p depletion experiment. At t_{50} they were still observed, but less frequently. Instead, numerous spherical mitochondria appeared distributed in unconnected manner throughout the cell (not shown). Selective degradation of organelles has been described to occur via microautophagy or macroautophagy.[12,17] Evidence of direct engulfment of mitochondrial material surrounded with cytosolic material within the concave membranes of vacuoles (Figure 5b, right panel) strongly suggests that microautophagy is occurring here. Macroautophagy cannot be excluded, but in contrast to microautophagy, a complete sequence of autophagosome formation events was not observed. None of the changes in vacuolar and mitochondrial morphology were observed in wild-type cells treated with dox (Figure 5c, left panel).

To test whether nigericin can rescue the mutant phenotypes of mitochondria and vacuoles, this K^+/H^+ ionophore was added to *MDM38*^{dox} cells grown for 25 h in presence of dox and then incubated in the presence of both drugs for further 4 h. As shown in Figure 5a (right panel), mitochondria appeared as elongated electron dense structures with abundant cristae, although these were swollen in comparison to those of mitochondria in wild-type cells. Moreover, the morphology of vacuoles was also restored, since the vacuolar membrane showed low electron density as shown by wild-type cells, no indentations and there were no larger inclusions visible in the vacuole (Figure 5c, left and right panels, respectively).

Taken together, these data reveal that Mdm38p depletion resulted in an early loss of K^+/H^+ exchange-mediated swelling capacity of mitochondria, loss of $\Delta\psi$ and in the extensive interaction of mitochondria with vacuoles, a phenomenon previously named mitophagy.[11,12] Reversion of these phenotypic features was observed following addition of the ionophore nigericin to growing cells. This strongly supports the notion that the loss of K^+/H^+ exchange activity is the primary cause for morphological changes of mitochondria, which in turn trigger the process of mitophagy.

Confocal microscopy of cells undergoing mitophagy induced by Mdm38p depletion. Figure 6 depicts mitochondrial structures observed by confocal microscopy in wild-type cells (Figures 6a–c) and in *mdm38*Δ mutant cells (Figures 6d–f) expressing GFP targeted to the mitochondrial matrix. In mutant cells (d–f) a large number of individual, spherical units were present instead of the highly branched mitochondrial network of wild-type cells (a–c). Similar structures were seen when GFP was directed to the outer mitochondrial membrane (data not shown). Accordingly, the distinct spherical units in *mdm38*Δ cells did not result from cristae constriction, but from a full breakdown of the mitochondrial network.

During Mdm38p depletion from *MDM38*^{dox} cells we observed that mitochondrial tubules initially became shorter and the regular distribution of elongated tubular networks throughout the cell cortex changed into crown-like networks of thick, but short branches surrounding the vacuole and were eventually fragmented into distinct spherical organelles (not shown). Table 1 indicates the percentage of cells exhibiting fragmented mitochondria observed over the period of Mdm38p downregulation in comparison to a strain constitutively expressing Mdm38p.

Simultaneous counterstaining of the vacuole membrane with the dye FM4-64 illustrated vacuolar membranes with indentations and pointed to some green and red overlaps after Mdm38p depletion, consistent with ongoing mitophagy. Parallel cultures of *MDM38*^{dox} cells, grown in the presence of dox and nigericin, did not show any indications of close proximity of vacuoles and mitochondria (not shown).

To monitor further the fate of mitochondria upon Mdm38p depletion, we made use of a biosensor targeted specifically to mitochondria by means of the citrate synthase targeting sequence. This biosensor consists of two fluorescent proteins, a pH-sensitive variant of GFP and a pH-insensitive variant of the RFP, DsRed. In the acidic environment of the vacuole (pH $\sim$5.5), the pH-sensitive GFP loses its fluorescence, whereas the red fluorescence expressed from the same construct is retained. Thus, this biosensor reports mitochondrial uptake by accumulation of red fluorescence within yeast vacuoles. For wild-type cells grown under non-starvation conditioned few cells show mitochondrial uptake; however, under starvation conditions mitochondrial uptake is dramatically enhanced (C Rosado, D Mijaljica, M Prescott and RJ Devenish, unpublished observations).

We co-transformed *MDM38*^{dox} with the biosensor construct pCS-G/RFP (this strain was denoted *MDM38*^{dox}*-G/RFP*) and monitored the changes in green and red fluorescence using confocal microscopy (Figure 7B). Time dependent depletion of Mdm38p was revealed in parallel by Western blotting (Figure 7A). The cells were grown to the early logarithmic stage for periods of 4, 10, 20, 25, 29, or 50 h in presence of dox, or dox and nigericin as indicated. Green fluorescence clearly documents the normal branched reticular network of mitochondria of wild-type cells. Red fluorescence colocalizes with green fluorescence as expected in wild-type cells, and there is little evidence for mitochondrial uptake into the

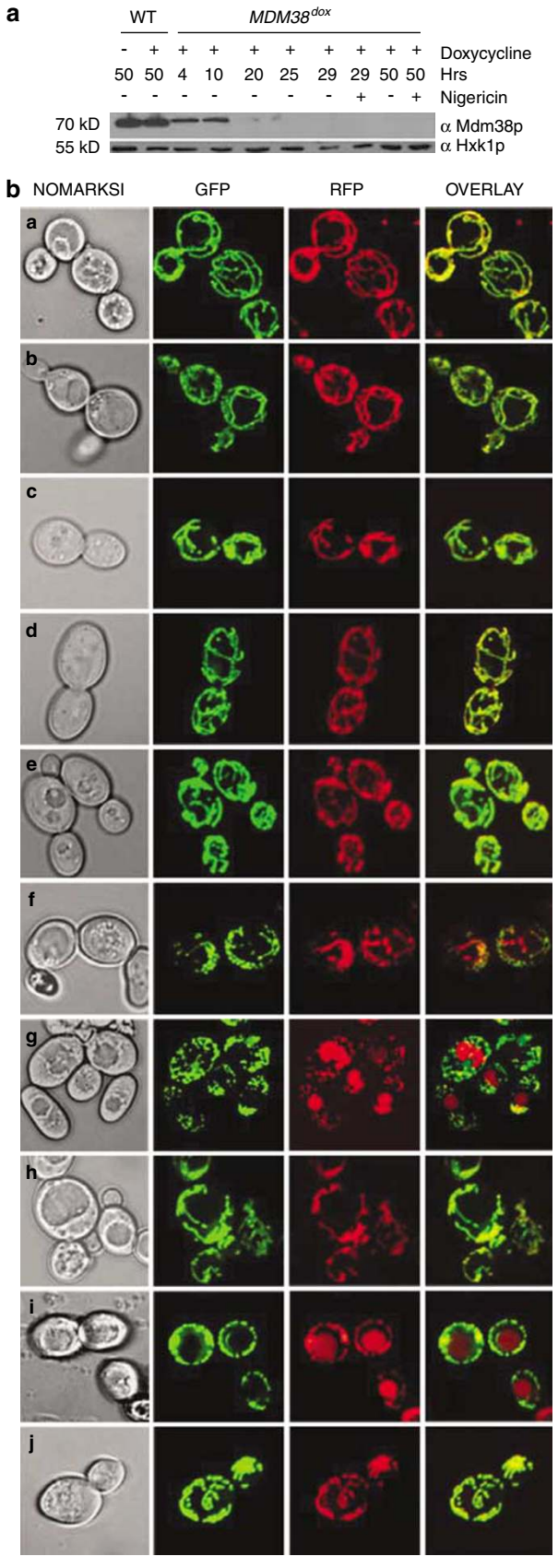

Table 1 Quantification of mitochondrial fragmentation upon doxycycline dependent repression of Mdm38p

Doxycycline	20 h	30 h	40 h	50–60 h
WT/GFP	<1	<5	<5	<6
MDM38^{dox}/GFP	8 ± 4	26 ± 11	37 ± 5	91 ± 2

Wild-type cells expressing the *tetO* promoter from the empty plasmid pCM189 (WT) and *MDM38*^{dox} cells, both carrying pYX232-mtGFP and maintained in logarithmic growth phase in the presence of 5 μl/ml doxycycline for the indicated time, were analyzed using conventional fluorescent microscopy. In each experiment the percentage of cells containing fragmented mitochondria from 10^3 *MDM38*^{dox} and WT cells was determined. The experiments were repeated separately at least three times. Data calculated from at least three independent experiments are presented as mean $\pm$ S.E.M.

vacuole since no red fluorescence is seen there (Figure 7B, panel a). Growth of wild-type cells in presence of dox for 50 h had no effect on the mitochondrial structure as can be seen in Figure 7B, panel b. In contrast, at early time points of growth of *MDM38*^{dox}*-G/RFP* cells in the presence of dox, the gradual alteration in mitochondrial morphology, from elongated to rounded forms, became evident. Similar to wild-type cells (Figure 7B, panel a), red fluorescence was first fully colocalized with green fluorescence as shown in the overlay image (Figure 7B, panels c–e). However, at a later time point (t_{25}), correlating to the loss of mitochondrial K^+/H^+ exchange activity and ongoing swelling, mitochondrial fragmentation became apparent and some fragmented organelles were found lacking green fluorescence but retaining red fluorescence (Figure 7B, panel f). Thereafter (t_{29} and t_{50}) significant accumulation of red fluorescence in vacuoles was detected, reflecting turnover of mitochondria in vacuoles (Figure 7B, panels g and i). In line with the EM data presented above, the appearance of some mitochondria showing red fluorescence only and thereafter of red fluorescence in vacuoles suggests that some mitochondria become acidic before being ingested. In a parallel experiment, *MDM38*^{dox}*-G/RFP* cells were grown for 29 and 50 h in the presence of dox with nigericin also present for the last 4 h. Remarkably, the mitochondria were fragmented to a much lesser extent and more strikingly, these cells did not display any accumulation of red fluorescence in the vacuoles (Figure 7B, panels h and j), suggesting little if any turnover of mitochondria was occurring. These results confirm that in the presence of the K^+/H^+ ionophore nigericin mitochondrial tubular networks have been re-established either by fusion of persisting spherical organelles, or from newly formed organelles, or both. Presumably, such

Figure 7 Mdm38p dependent mitochondrial turnover. (**A**) Western blot detection of Mdm38p during dox-dependent growth in wild type expressing the *tetO* promoter from the empty plasmid pCM189 and G/RFP from the plasmid pCS-G/RFP (WT) and in *MDM38*^{dox}–G/RFP cells. Whole cell extracts corresponding to 1 ml ($OD_{600} = 4$) were separated by 12.5% SDS-PAGE and probed with antiserum against Mdm38p. Blot probed with antiserum against Hxk1p served as a loading control. (**B**) Confocal microscopy. Control wild-type strain expressing the empty pCM189 and pCS-G/RFP in absence (**a**) or in presence of dox (**b**). *MDM38*^{dox} cells transformed with the plasmid pCS-G/RFP and grown for 4, 10, 20, 25, 29, or 50 h under Mdm38p depletion conditions (**c**–**g**, and **i**). Cells from the same pre–culture as in (**g** and **i**), but grown for 29 or 50 h in the presence of both dox and nigericin added for the last 5 h of the growth, respectively (**h** and **j**)

mitochondria are no longer marked for vacuolar degradation even in the absence of Mdm38p.

To learn whether mitophagy induced by dysfunctional mitochondria contributes to cell survival, aliquots of logarithmic growth phase cells taken from each time point of Mdm38p depletion were stained with the vital stain Trypan blue and the percentage of dead cells was evaluated. Both, wild type and *MDM38*^{dox}*-G/RFP* cells exhibited a cell death rate of 0.5–3% per generation. Thus, induction of mitophagy (clearly observed from t_{25} on) has no significant effect on cell viability. Interestingly, we noticed that Mdm38p depletion had a strong negative effect on survival of cells in stationary growth phase. Cells grown for 50 h in presence of dox were kept in the original galactose-containing growth medium and incubated with shaking at 28°C for a week. Every day samples were taken and stained with Trypan blue. Counting of Trypan blue-positive cells indicated a significant decrease in the survival rate of Mdm38p depleted cells in comparison to wild-type cells (Figure 8).

Fragmentation and autophagic degradation of *mdm38*Δ mitochondria require the presence of Dnm1p. As described previously, the dynamin-related GTPase Dnm1p mediates scission of the outer mitochondrial membrane. Mitochondrial membranes in the *dnm1*Δ strain have been shown to be collapsed into one or more long tubular structures near the cell cortex and often a planar 'net' of interconnected tubules.[19,20] We addressed the question whether fragmentation of *mdm38*Δ mitochondria could be restored by changing the balance towards reduced fission or enhanced fusion. We first constructed a *dnm1*Δ*mdm38*Δ strain expressing the mitochondrial targeted GFP and then examined the mitochondrial network. Confocal microscopy of *dnm1*Δ*mdm38*Δ cells expressing mitochondrially targeted GFP revealed the presence of giant mitochondrial spheres without any obvious tubulation. The *dnm1*Δ mutation thus prevented the fragmentation of mitochondria into a larger number of spherical units typical of *mdm38*Δ single mutant cells. Simultaneous counterstaining of vacuolar membranes with the dye FM4-64 (not shown), or expression of p*CS-G/RFP* in *dnm1*Δ*mdm38*Δ cells revealed that *dnm1*Δ suppressed *mdm38*Δ induced mitophagy (Figure 9a). Transmission electron microscopy of *dnm1*Δ*mdm38*Δ cells (Figure 9b and c) confirmed the presence of giant mitochondrial spheres. Formation of these giant spheres is assumed to reflect osmotic swelling of mitochondria due to the lack of Mdm38p combined with a fission defect due to the *dnm1*Δ mutation. The lack of association between mitochondria and vacuoles in the double mutant suggests that mitophagy is prevented by the fission defect and that fragmentation of mitochondria may be a prerequisite for the degradation process. Interestingly, growth of *dnm1*Δ*mdm38*Δ cells was much reduced compared to *mdm38*Δ cells, both on fermentable and non-fermentable substrates (not shown). Western blotting revealed only traces of Cox2 protein and reduced amounts of ATPase F1β subunit in *dnm1*Δ*mdm38*Δ mitochondria (Supplementary Figure S1A and B). This is consistent with the near total absence of cristae structures.

Finally, we asked if mitochondrial fragmentation and mitophagy could be compensated by enhancing fusion activity. Therefore, we overexpressed Fzo1p or Mgm1p, both proteins mediating mitochondrial fusion, in *mdm38*Δ cells. Neither protein could counteract the process of mitochondrial fragmentation and mitophagy or rescue the *mdm38*Δ *petite* phenotype (data not shown), indicating that fragmentation of *mdm38*Δ mitochondria is not caused by low activity of proteins that promote mitochondrial fusion.

Discussion

Conditional shutdown of *MDM38* gene expression has been used here to discriminate between primary and secondary phenotypic effects resulting from the loss of Mdm38p in yeast

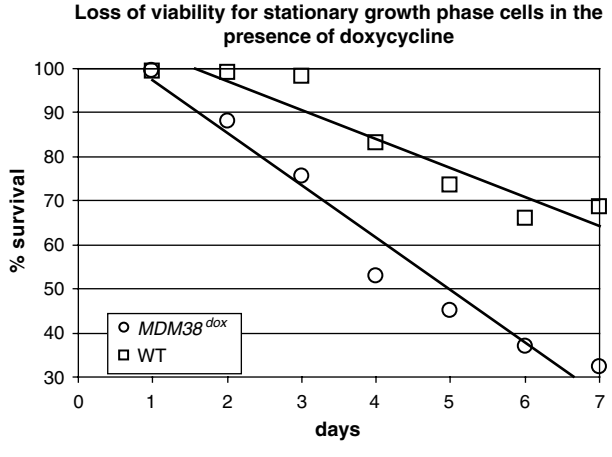

Figure 8 Cell survival in stationary phase. Wild type (WT) and Mdm38p-depleted cells (*MDM38*^{dox}) were kept in stationary phase for 7 days in presence of 5 μg/ml dox. Cell viability was determined each day using Trypan blue staining and counting of 10^3 cells under light microscopy. % survival is the percentage of Trypan-blue-negative (unstained) cells. The results present the average of three different experiments

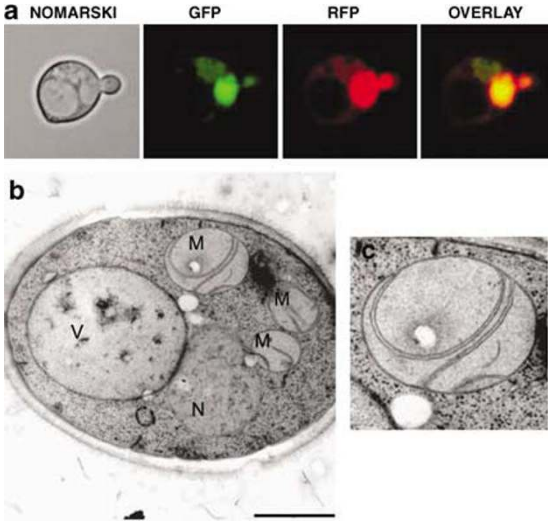

Figure 9 Structure of *dnm1*Δ *mdm38*Δ cells. (**a**) Nomarski and fluorescence microscopy *of dnm1*Δ*mdm38*Δ cells expressing pCS-G/RFP. (**b**) EM of *dnm1*Δ*mdm38*Δ cells grown to early logarithmic phase in YPGal. V, vacuole; M, mitochondrion; N, nucleus. Scale bar, 2 μM. (**c**) Details of (**b**)

cells. While the pattern of mitochondrially synthesized proteins as well as of cytochrome spectra remained unaffected even after prolonged Mdm38p depletion, mitochondrial K^+/H^+ exchange activity diminished with the loss of Mdm38p. Accordingly, we conclude that this is the predominant and only known phenotype immediately resulting from Mdm38p depletion. Strong support for this conclusion comes from our observation that nigericin, a K^+/H^+ ionophore, restores growth of Mdm38p depleted cells on non-fermentable media. Loss of mitochondrially synthesized proteins,[13] therefore, is not a primary phenotypic feature of Mdm38 depletion.

Loss of K^+/H^+ exchange activity in *mdm38*Δ cells resulted in mitochondrial K^+ overload and osmotic swelling.[6,9] As shown here by EM and confocal microscopy, these events were paralleled by the conversion of the tubular mitochondrial network into many distinct spheres and their association with the yeast vacuole. Moreover, the vacuolar membrane was found to be considerably thickened and to exhibit indentations all over. This pathway has features similar to those recently described, where the vacuolar membrane exhibited concave indentations associated with microautophagy of mitochondria.[11,16] It is unclear at present how selective this microautophagy might be. However, recent studies implicate mitochondrial membrane depolarization and swelling of the matrix compartment in the onset of selective macroautophagic degradation processes.[21,22]

Here, we made use of electron microscopy and a novel biosensor composed of a pH-sensitive GFP and a pH-insensitive RFP, targeted to mitochondria. Upon Mdm38p depletion in logartithmically growing cells, we found red fluorescence associated with vacuoles indicative of the uptake of mitochondria into vacuoles. Addition of nigericin, a K^+/H^+ ionophore, to growing *mdm38*Δ cells depleted for Mdm38p essentially reverted the appearance of mitochondria as well as of vacuoles within a few hours. There were no longer any indications of ongoing mitophagy. Thus, autophagic degradation of mitochondria in Mdm38p-depleted cells clearly correlates with the loss of K^+/H^+ exchange activity.

For the first time our data show that a mutation-induced dysfunction of mitochondria, without any externally added drugs or physiological stresses, can trigger extensive mitophagy. In previous experiments, the onset of mitophagy had been attributed to the impairing of the mitochondrial electrochemical transmembrane potential.[11] Mdm38p-depleted cells showed a reduction in $\Delta\psi$, but two observations suggested that this was not sufficient to trigger fragmentation of the mitochondrial network and mitophagy. First, growth of *mdm38*Δ cells in the presence of oligomycin restored $\Delta\psi$, but not the tubular reticulum of mitochondria (not shown). Second, mutants lacking Cox4 (*cox4*Δ) or having very low amounts of Cox2 only (*dnm*Δ*mdm38*Δ, Supplementary Figure S1), show a similar reduction in $\Delta\psi$ as *mdm38*Δ cells and show no signs of mitophagy (data not shown). Accordingly, we conclude that osmotic swelling of Mdm38p-depleted cells is sufficient to massively induce mitophagy, provided that fragmentation of the mitochondrial reticulum is not inhibited.

Induction of mitophagy by Mdm38p depletion had no significant effect on cell viability under logarithmic growth conditions. Ultrastructure analysis of cells by electron microscopy revealed enhanced abundance of spherical mitochondria after prolonged (t_{50}) depletion of Mdm38p. Presumably, in logarithmic growth, ongoing mitochondrial proliferation counterbalances degradation. In stationary phase, however, Mdm38p depleted cells had a significantly reduced survival rate as compared to wild-type cells, suggesting a synthetic effect of mitophagy and stationary phase induced autophagy. Thus, Mdm38p is required for enhanced survival of cells in stationary phase, and mitophagy in stationary phase is likely involved in a cell death program.

Overexpression of proteins of the fusion machinery (Mgm1p, Fzo1p), had no significant effect on *mdm38*Δ mitochondrial morphology, or mitophagy. By contrast, deletion of *DNM1*, a gene with a central role in mitochondrial fission,[23] generated a mitochondrial phenotype combining the features of the *dnm1*Δ mutant and the *mdm38*Δ mutant. These *mdm38*Δ*dnm1*Δ double mutant cells contained one or few individual giant mitochondrial spheres which we interpret as resulting from osmotic swelling of mitochondria which continue to fuse but lack fission activity. Interestingly, a block of fission by the *dnm1*Δ mutation prevented mitochondrial fragmentation and also mitophagy. Thus, it appears that induction of mitophagy in *mdm38*Δ cells requires the mitochondrial reticulum to be capable of undergoing fission. Our experimental data provide the first evidence in support of the idea that formation of discrete mitochondrial units allows the cell to rid itself of damaged parts of the mitochondrial network rather than the whole network.[12] Support for this idea is also provided by the studies of Lemasters,[22] concerning selective mitophagy in hepatocytes, where mitochondria are generally found as discrete spheres rather than as a reticulum.

Materials and Methods

Yeast strains, plasmids and media. The *Saccharomyces cerevisiae* strain W303 (ATCC no. 201239) served as wild-type strain. The null mutant *mdm38*Δ was constructed from W303 by replacement of *MDM38* with *HIS3* as described previously in Nowikovsky *et al*.[6] To generate the *mdm38*Δ*dnm1*Δ double deletion strain, *mdm38*Δ was crossed with the deletion strain *dnm1*Δ obtained from sporulation of W303 *mgm1*Δ*dnm1*Δ generously provided by Sesaki *et al*.[24]

Culturing of yeast was performed according to standard protocols at 30°C on yeast media, including YPD (2% glucose), YPG 2% (glycerol), YPGal (2% galactose), YPRaf (2% raffinose), SRaf (2%Raf) and SGal (2% galactose), prepared as described previously,[25] except for SGal liquid medium which was supplemented with 2 mM adenine. Yeast transformations were performed as described previously.[26] For all experiments except the one shown in Figure 2, all strains (but not the cox2/3Δ mutants) were grown in galactose containing-media, since galactose is a fermentative carbon source that does not repress mitochondria like glucose. Dox was used when indicated at a concentration of 5 μg/ml. All experiments described in this study were carried out with cultures of cells kept in the logarithmic phase of growth unless otherwise stated. Exponential cultures were diluted as appropriate if grown over periods longer than overnight.

Mitochondrial DNA mutants PTY cox2Δ, PTY *cox3*Δ (G. Wiesenberger) fail to express the Cox2, or Cox3 protein, respectively and were grown on YPRaf. To express *MDM38* under a regulated promoter, we constructed an *mdm38*Δ strain expressing Mdm38p from a dox repressible (*tetO*) promoter. For this purpose, *MDM38* was amplified from YCp-*MDM38-HA*[6] with the primers 5′-TAATAT**GGATCC**ATGTTGAATTTCGCATCAAGAGCG-3′ and 5′-ATATAT**GGCCCTAGCGGCC**TCAGCACTGAGCAGCGTAATCTGG-3′ and the Bam*H*1–*Sfi1* fragment was inserted into the respective sites of the vector pCM189,[27] yielding pCM189-*MDM38*-HA.

The biosensor construct pCS-G/RFP used to follow mitochondrial uptake into vacuoles was constructed by sequential addition of three DNA sequence cassettes into the yeast multi-copy expression vector pAS1NB,[28] having *PGK1* transcription

control sequences and *LEU2* selectable marker. The sequence cassettes encoded the following components: (1) the RFP component retrieved by PCR from pQE31-DsRed.T3;[29] (2) the GFP component retrieved by PCR from pGEX-2 T carrying the ecliptic pHluorin;[30] and (3) the first 55 amino acids of the yeast citrate synthase precursor polypeptide amplified by PCR from yeast genomic DNA.[31]

Visualization of mitochondria with mitochondrial matrix targeted GFP expressed from the constitutive TPI (triosephosphate isomerase) promoter was achieved by use of the plasmid pYX232-mtGFP.[18]

***In vivo* labeling of mitochondrial translation products.** *In vivo* pulse labeling was performed according to Fox *et al.*[32] Briefly, wild-type expressing the empty plasmid pCM189 and *MDM38*^{dox} cells were pre-grown in SGal medium containing dox (5 μg/ml), wild type and *mdm38*Δ in YPGal. Nigericin (2 μM) was added as indicated. Control *mit*$^-$ strains (*cox2*Δ, *cox3*Δ) were grown in YPRaf. Cells taken from precultures were transferred to synthetic medium lacking methionine and incubated for 3 h in presence or absence of dox as indicated. After addition of cycloheximide (150 μg/ml) cells were labeled with ^{35}S-methionine (8 μl/ml of a 5 mMCi stock, Amersham) and incubated for 30 min with agitation. Reactions were chased with unlabeled methionine (4 mM) for 10 and 120 min. Whole cell proteins were precipitated with trichloroacetic according to Westermann,[33] separated by 16% SDS-PAGE and visualized by autoradiography.

Isolation of mitochondria. Yeast mitochondria from cultures grown exponentially in galactose-containing media were isolated as described in Nowikovsky *et al.*[6]

Western blotting. Yeast cells were grown in SGal in absence or presence of 5 μg/ml dox as indicated. Cultures were re-diluted as required to keep them in logarithmic growth phase. Total cell extracts were analyzed using 12.5% polyacrylamide gels unless indicated otherwise. Proteins were transferred to a nitrocellulose membrane and analyzed using primary antibodies to HA (1 : 200;[34]), Hexokinase-1 (1 : 15 000; Biotrend), GFP (1 : 2000; Roche), Mdm38p (1 : 200; provided by P. Rehling) in PBS-T plus 5% dry milk. Proteins were visualized by incubation with the mouse or rabbit secondary antibody conjugated to horseradish peroxidase (1 : 10 000; Molecular Probes, or 1 : 15 000; Sigma, respectively) in PBS-T plus 5% dry milk, followed by ECL (Pierce).

Measurement of K^+/H^+ exchange activities. Light scattering experiments were performed as previously described in Nowikovsky *et al.*[6]

Determination of mitochondrial $\Delta\psi$. Isolated yeast mitochondria (0.5 mg protein) were incubated in the presence of 0.5 mM ATP, 0.2% succinate and 0.01% pyruvate with 0.5 μM JC-1 (5,5′,6,6′-tetrachloro-1,1′,3,3′-tetraethylbenzimidazolo-carbocynine iodide, Molecular Probes) for 7 min at room temperature in the dark. The intensity changes of the monomeric form (low energy, 540 nm) and of the multimeric form (high energy, 590 nm) were recorded with the Scan mode of the Perkin Elmer LS55 luminescence photometer. Data collection was carried out with FL WinLab4.0. For calibration, aliquots of the same preparation were hyperpolarized with 1 μM nigericin (Sigma) and depolarized with 1 μM carbonylcyanide-p-trifluoromethoxyphenylhydrazone (FCCP, Sigma). A calibration curve was calculated for every single measurement and applied to correlate the $\Delta\psi$ expressed as a percentage of the maximum and the minimum obtained by hyperpolarization and depolarization, respectively.

Microscopy. pVT100U-mtGFP, pYX232-mtGFP,[18] pCS-G/RFP (C Rosado, M Prescott, and RJ Devenish, unpublished) or 5 μM rhodamine B hexyl ester (Molecular Probes) served to label mitochondria. Vacuoles were stained with FM4-64 in a final concentration of 10 μM (Molecular Probes). Classification of the morphotype of cells in logarithmic growth phase was performed with hidden identity by standard fluorescence microscopy on Axioplan 2 with a 63 oil immersion objective (Zeiss Plan Apochromat). Confocal images were captured with a Zeiss Axiowert LSM 510 microscope. The excitation wavelength for GFP and FM4-64/dsRed was 488 and 543 nm, respectively. Images were acquired in multitrack Z stack and projected with LSM5 Image Browser.

Electron microscopy. Cells were harvested at early logarithmic growth phase ($OD_{600} = 0.5$). For cryofixation, cell pellets were introduced to flat sample holders of an EMPACT high-pressure freezer (LEICA Microssystems, Austria). With the help of a loading station, the flat specimen holders were placed in a sample holder pod and tightly sealed. The samples were frozen at a pressure of about 2000 bar, as described previously for specimens of mammalian tissues.[35] Following freezing, the flat specimen holders were separated from the pods under liquid nitrogen and transferred to a LEICA AFS freeze substitution system (LEICA Microsystems, Austria). Freeze-substitution was as described elsewhere.[36] In short, samples were substituted in acetone containing 2% OsO_4 for 4 days at -90°C, followed by warming and embedding in epoxy resin (Agar 100). Thin sections were cut with an Ultracut S ultramicrotome (LEICA Microsystems, Austria), mounted on copper grids with Formvar support film, counterstained with uranyl acetate and lead citrate and examined at 80 kV in a JEOL JEM-1210 electron microscope. Images were acquired using a digital camera Morada for the wide-angle port of the TEM and analySIS FIVE software (Soft Image System).

Trypan blue staining. Cells were collected and stained with Trypan blue (Gibco BRL) for 15 min at room temperature. Unstained cells (alive) and blue cells (dead) were visualized and counted under light microscopy.

Acknowledgements. We thank Hiromi Sesaki (Baltimore) for strains, Gottfried Schatz (Basel), Benedikt Westermann (Bayreuth), Peter Rehling (Freiburg) for generously provided antibodies, Mirjana Iliev for excellent technical assistance, Gerlinde Wiesenberger for strains, helpful discussion and comments. This work was supported by the Austrian Science Fund (FWF).

1. Okamoto K, Shaw JM. Mitochondrial morphology and dynamics in yeast and multicellular eukaryotes. *Annu Rev Genet* 2005; **39**: 503–536.
2. Meeusen SL, Nunnari J. How mitochondria fuse. *Curr Opin Cell Biol* 2005; **17**: 389–394.
3. Boldogh IR, Pon LA. Interactions of mitochondria with the actin cytoskeleton. *Biochim Biophys Acta* 2006; **1763**: 450–462.
4. Frieden M, James D, Castelbou C, Danckaert A, Martinou JC, Demaurex N. Ca(2+) homeostasis during mitochondrial fragmentation and perinuclear clustering induced by hFis1. *J Biol Chem* 2004; **279**: 22704–22714.
5. Dimmer KS, Fritz S, Fuchs F, Messerschmitt M, Weinbach N, Neupert W *et al.* Genetic basis of mitochondrial function and morphology in *Saccharomyces cerevisiae*. *Mol Biol Cell* 2002; **13**: 847–853.
6. Nowikovsky K, Froschauer EM, Zsurka G, Samaj J, Reipert S, Kolisek M *et al.* The LETM1/YOL027 gene family encodes a factor of the mitochondrial K^+ homeostasis with a potential role in the Wolf-Hirschhorn syndrome. *J Biol Chem* 2004; **279**: 30307–30315.
7. Zollino M, Lecce R, Fischetto R, Murdolo M, Faravelli F, Selicorni A *et al.* Mapping the Wolf–Hirschhorn syndrome phenotype outside the currently accepted WHS critical region and defining a new critical region, WHSCR-2. *Am J Hum Genet* 2003; **72**: 590–597.
8. Scorrano L. Proteins that fuse and fragment mitochondria in apoptosis: con-fissing a deadly con-fusion? *J Bioenerg Biomembr* 2005; **37**: 165–170.
9. Froschauer E, Nowikovsky K, Schweyen RJ. Electroneutral K^+/H^+ exchange in mitochondrial membrane vesicles involves Yol027/Letm1 proteins. *Biochim Biophys Acta* 2005; **1711**: 41–48.
10. Szyrach G, Ott M, Bonnefoy N, Neupert W, Herrmann JM. Ribosome binding to the Oxa1 complex facilitates co-translational protein insertion in mitochondria. *EMBO J* 2003; **22**: 6448–6457.
11. Priault M, Salin B, Schaeffer J, Vallette FM, di Rago JP, Martinou JC. Impairing the bioenergetic status and the biogenesis of mitochondria triggers mitophagy in yeast. *Cell Death Differ* 2005; **12**: 1613–1621.
12. Mijaljica D, Prescott M, Devenish RJ. Different fates of mitochondria: alternative ways for degradation? *Autophagy* 2007; **3**: 4–9.
13. Frazier AE, Taylor RD, Mick DU, Warscheid B, Stoepel N, Meyer HE *et al.* Mdm38 interacts with ribosomes and is a component of the mitochondrial protein export machinery. *J Cell Biol* 2006; **172**: 553–564.
14. Welihinda AA, Trumbly RJ, Garlid KD, Beavis AD. On the regulation of Na+/H^+ and K^+/H^+ antiport in yeast mitochondria: evidence for the absence of an Na(+)-selective Na+/H^+ antiporter. *Biochim Biophys Acta* 1993; **1144**: 367–373.
15. Kissova I, Plamondon LT, Brisson L, Priault M, Renouf V, Schaeffer J *et al.* Evaluation of the roles of apoptosis, autophagy and mitophagy in the loss of plating efficiency induced by Bax-expression in yeast. *J Biol Chem* 2006; **281**: 36187–36197.
16. Kissova I, Salin B, Schaeffer J, Bhatia S, Manon S, Camougrand N. Selective and non-selective autophagic degradation of mitochondria in yeast. *Autophagy* 2007; **3**: 329–336.
17. Monastyrska I, Klionsky DJ. Autophagy in organelle homeostasis: Peroxisome turnover. *Mol Aspects Med* 2006; **27**: 483–494.
18. Westermann B, Neupert W. Mitochondria-targeted green fluorescent proteins: convenient tools for the study of organelle biogenesis in *Saccharomyces cerevisiae*. *Yeast* 2000; **16**: 1421–1427.
19. Bleazard W, McCaffery JM, King EJ, Bale S, Mozdy A, Tieu Q *et al.* The dynamin-related GTPase Dnm1 regulates mitochondrial fission in yeast. *Nat Cell Biol* 1999; **1**: 298–304.

20. Shaw JM, Nunnari J. Mitochondrial dynamics and division in budding yeast. *Trends Cell Biol* 2002; **12**: 178–184.
21. Bradshaw PC, Pfeiffer DR. Loss of NAD(H) from swollen yeast mitochondria. *BMC Biochem* 2006; **7**: 3.
22. Lemasters JJ. Selective mitochondrial autophagy, or mitophagy, as a targeted defense against oxidative stress, mitochondrial dysfunction, and aging. *Rejuvenation Res* 2005; **8**: 3–5.
23. Naylor K, Ingerman E, Okreglak V, Marino M, Hinshaw JE, Nunnari J. Mdv1 interacts with assembled dnm1 to promote mitochondrial division. *J Biol Chem* 2006; **281**: 2177–2183.
24. Sesaki H, Southard SM, Yaffe MP, Jensen RE. Mgm1p, a dynamin-related GTPase, is essential for fusion of the mitochondrial outer membrane. *Mol Biol Cell* 2003; **14**: 2342–2356.
25. Sherman F. Getting started with yeast. *Methods Enzymol* 1991; **194**: 3–21.
26. Gietz RD, Woods RA. Transformation of yeast by lithium acetate/single-stranded carrier DNA/polyethylene glycol method. *Methods Enzymol* 2002; **350**: 87–96.
27. Gari E, Piedrafita L, Aldea M, Herrero E. A set of vectors with a tetracycline-regulatable promoter system for modulated gene expression in *Saccharomyces cerevisiae*. *Yeast* 1997; **13**: 837–848.
28. Prescott M, Nowakowski S, Gavin P, Nagley P, Whisstock JC, Devenish RJ. Subunit gamma-green fluorescent protein fusions are functionally incorporated into mitochondrial F1F0-ATP synthase, arguing against a rigid cap structure at the top of F1. *J Biol Chem* 2003; **278**: 251–256.
29. Bevis BJ, Glick BS. Rapidly maturing variants of the Discosoma red fluorescent protein (DsRed). *Nat Biotechnol* 2002; **20**: 83–87.
30. Miesenbock G, De Angelis DA, Rothman JE. Visualizing secretion and synaptic transmission with pH-sensitive green fluorescent proteins. *Nature* 1998; **394**: 192–195.
31. Gavin P, Devenish RJ, Prescott M. An approach for reducing unwanted oligomerisation of DsRed fusion proteins. *Biochem Biophys Res Commun* 2002; **298**: 707–713.
32. Fox TD, Folley LS, Mulero JJ, McMullin TW, Thorsness PE, Hedin LO *et al.* Analysis and manipulation of yeast mitochondrial genes. *Methods Enzymol* 1991; **194**: 149–165.
33. Westermann B, Herrmann JM, Neupert W. Analysis of mitochondrial translation products *in vivo* and in organello in yeast. *Methods Cell Biol* 2001; **65**: 429–438.
34. Bui DM, Gregan J, Jarosch E, Ragnini A, Schweyen RJ. The bacterial magnesium transporter CorA can functionally substitute for its putative homologue Mrs2p in the yeast inner mitochondrial membrane. *J Biol Chem* 1999; **274**: 20438–20443.
35. Reipert S, Fischer I, Wiche G. High-pressure freezing of epithelial cells on sapphire coverslips. *J Microsc* 2004; **213** (Part 1): 81–85.
36. Studer D, Graber W, Al-Amoudi A, Eggli P. A new approach for cryofixation by high-pressure freezing. *J Microsc* 2001; **203** (Part 3): 285–294.

Supplementary Information accompanies the paper on Cell Death and Differentiation website (http://www.nature.com/cdd)